JULY 12–16
2020 VIRTUAL
JOINT AAPM | COMP MEETING
EASTERN TIME [GMT-4]

Prompt Gamma Spectroscopy of Metallic Implants in Proton Therapy: a Monte Carlo Study

Chun-Yu Liu[1], Chung-Hao Su[2], Yueh Chiang[1], Chung-Chi Lee[1], Tsi-Chian Chao[1], Hsin-Hon Lin[2*]

1 Department of Medical Imaging and Radiological Sciences, Chang Gung University, Taoyuan City, Taiwan
2 Institute for Radiological Research, Chang Gung University/Chang Gung Memorial Hospital, Taoyuan City, Taiwan

INTRODUCTION

Particle therapy, unlike conventional photon therapy, has a low entrance dose, followed by a region of uniform high dose (the spread-out Bragg peak) at the tumor, then a steep falloff to zero doses. These characteristics make possible a substantial dose reduction to the normal tissues while maximizing the dose to the tumor and give proton therapy an inherent advantage over photon therapy. However, due to the range uncertainty, a safety margin of 3.5% of the proton range plus an additional setup uncertainty is considered to ensure adequate tumor control probability.

Prompt gamma (PG) measurement is one of the in-vivo range verification techniques. The production of the prompt gamma signal comes from the de-excitation nucleus during the particle therapy[1]. By detecting the intensity of specific energy peak, one can find the correlation between the intensity of several spectral lines and the placement of Metallic Implants at different depths of the proton beam.

AIM

The purpose of the study is to explore the correlation between the intensity of several spectral lines and the placement of Metallic Implants at different depths of the proton beam.

METHODS

GATE (Geant4 application for tomographic emission), a Monte-Carlo simulation program is used. In this work, we implanted an metallic marker (Silver and Gold) in a cylindrical PMMA phantom (20 cm in diameter, 30 cm in length) at different depth (Fig.1). The phantom irradiated with 150, 180 and 200 MeV proton, and metallic marker are placed at $R50_p$ to $R50_d$ (depth at 50% maximum dose in proximal/distal side) and the proximal region. For each simulation, 2 x 10^7 protons are used. Two physics lists of QGSP_BIC_HP_EMY and QGSP_BIC_AllHP_EMY were considered[2], where one is recommended for medical application, and another for high precision neutron simulation.

Two types of spectra were scored in each simulation: One was the detection of a HPGe detector, where the energy resolution we set as 0.177% with a reference energy of 662 keV; the other is the detection of an ideal detector (perfect absorption and resolution) using the recording of phase space. For each spectrum, the neuron-induced background or scattered gammas were removed using the statistics-sensitive non-linear iterative peak-clipping (SNIP) algorithm[3]. After the background subtraction, each "interested" PG energy peak is fitted by Gaussian function, yielding the integral of the intensity curve. The integral is as follows: $\int_{E_{PG}-3\sigma}^{E_{PG}+3\sigma} g(E)dE$

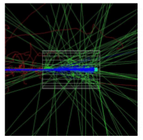

Fig.1 The visualization of GATE/GEANT4 particle trajectories along the proton irradiation of PMMA phantom and metallic implant (cyan). Proton, electrons and photons are shown in blue, red and green, respectively.

RESULTS

The influence of two physics lists (QGSP_BIC_HP and QGSP_BIC_AllHP) on the PG production was compared. The phase space file record the creation process of the gamma ray that enters the phase space volume. The useful PG for proton range monitoring is induced by the proton inelastic collision. In the QGSP_BIC_AllHP model, the PG induced by proton inelastic reaction spreads out and became easily be mistaken for a continuous background (Fig. 2(a) blue line). In comparison, the QGSP_BIC_HP model presents a distinct bell-shaped distribution caused by the Doppler broadening effect. The main PG peak (i.e. 4.44MeV form $^{12}C^*_{4.44} \rightarrow {}^{12}C_{g.s}$, 6.13MeV from $^{16}O^*_{6.13} \rightarrow {}^{16}O_{g.s}$) shows the Doppler broadening effect (Fig. 2(b)), which has been observed in many measurement experiments. After the evaluation of two physics lists, the QGSP_BIC_HP model was selected for the study based on the following reasons: (1) QGSP_BIC_HP model shows a similar result with the PG measurement; (2) PG peaks from the AllHP model were hard to be defined and interpreted.

The metallic implants (silver and gold) had its unique PG spectrum (Fig. 3). The PG peaks of 635 keV and 1405 keV for gold[4] and 633 keV for sliver[5] were selected. The relative intensity of the peaks had a similar trend with the Bragg peak, each of them showed the highest point near the R_{100} (range at maximum dose), then fall with sharp steepness. The distance between the Bragg peaks and highest intensity of PG curve about 5 to 8 mm, depending on the PG cross-section in the low energy area (Fig. 4).

Simulated detector spectra and energy resolution were illustrated in Fig. 5. We compared the HPGe, CZT, and LYSO for different energy resolutions. In our research, the HPGe and CZT were able to identify the sliver marker's PG peak in PMMA phantom. However, most of the PG peaks were smoothed because of the low energy resolution.

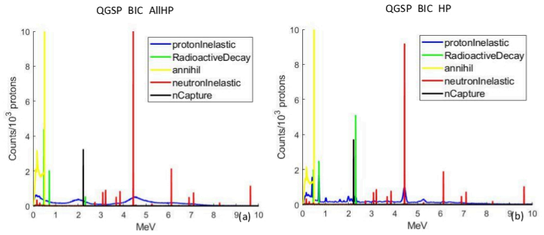

Fig. 2 The PMMA phantom spectra of AllHP and HP model. The PG creation process were classified as (1) proton inelastic (2) radioactive decay (3) neutron inelastic (4) neutron capture.

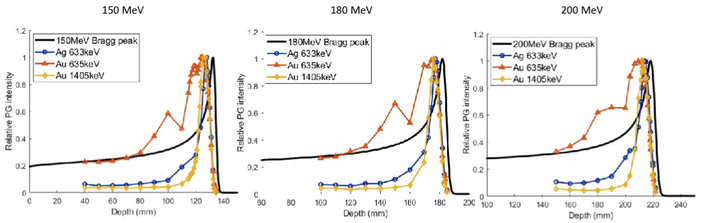

Fig. 4 PG intensity curve with the Bragg peak position.

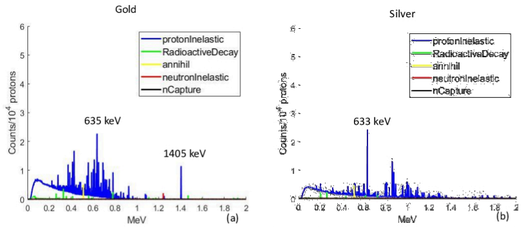

Fig. 3 The spectra from metallic implants. (a) Two peaks from the gold marker, 635 keV and 1405 keV, were chosen: the former was the highest peak, while the latter one would not be merged by other peak. (b) 633 keV is the highest peak in silver spectrum , and it had high cross-section in low energy region.

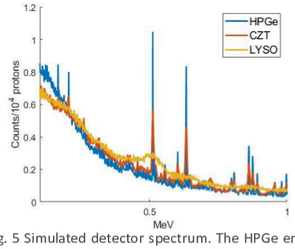

Fig. 5 Simulated detector spectrum. The HPGe energy resolution is 0.177% at 662 keV, the simulated CZT detector is 1.1% at 662 keV. LYSO is 14.6% at 511keV.

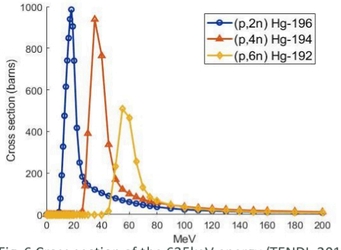

Fig. 6 Cross section of the 635keV energy (TENDL-2019, TALYS).

DISCUSSIONS & CONCLUSIONS

The proton inelastic spectrum in the QGSP_BIC_AllHP physics list shows a smoothed signal, and most of the PG energy peaks could not be identified from the spectrum. In QGSP_BIC_HP physics list, 4.44 MeV from $^{12}C^*$, 5.27 MeV from 15N* and 6.13 MeV from $^{16}O^*$ can be clearly identified. We inferred that the neutron probability inside QGSP_BIC_AllHP model dominates the whole simulation, and suppressed the proton inelastic interaction probability. Both the metallic implants and PMMA phantom show fewer amounts of PG peaks in this model used. From our point of view, the QGSP_BIC_AllHP model is not suitable in the prompt gamma simulation until it modifies the probability of proton signal. The PG intensity curves were influenced by three factors: (1) proton fluence, (2) proton energy and (3) cross section of the target. The energy peak of 635 keV from the PG spectrum of the gold holds three high intensities at different depths. Due to the Doppler broadening effect, these closed energy peaks were merged. Therefore, the 635 keV composed of three closed energy peaks in different depths. The peaks produced by Au^{197} (p,2n) Hg^{196*}, Au^{197}(p,4n) Hg^{194*} and Au^{197}(p,6n) Hg^{192*} reaction, the PG energy of three reactions were 635.5, 636.5 and 634.8 keV. The cross-section of each reaction was illustrated in Fig. 6.

Our results indicated that the intensity of the gamma lines pertaining to the metallic implants is correlated with the placement of Metallic Implants at the depths of the proton beam. This correlation had the potential to help estimate the residual range for range verification.

REFERENCES

[1] **Kozlovsky B et al** *2002*. Nuclear deexcitation gamma-ray lines from accelerated particle interactions. *Astrophys. J. Suppl. Ser. 141 523–41*

[2] **A Schumann et al**. *2015*. Simulation and experimental verification of prompt gamma-ray emissions during proton irradiation. *Phys. Med. Biol. 60 4197*

[3] **M Morhác et al**. *2008*. Peak clipping algorithms for background estimation in spectroscopic data. *Appl. Spectrosc. 2008, 62, 91–106.*

[4] **Huang**. *2006*. Nuclear data sheets for A = 196*. *Nucl. Data Sheets 108, 1093–1286.*

[5] **A. Khaliel et al**. *2017*. First cross-section measurements of the reactions ^{107,109}Ag(p,γ)^{108,110}Cd at energies relevant to the p process. *Phys. Rev. C 96, 035806*

ACKNOWLEDGEMENTS

The authors would like to thank Institute for Radiological Research of Chang Gung University/Chang Gung Memorial Hospital (Contract No. CIRPD1E0041) for financially supporting this research. The work was also supported in part by the Ministry of Science and Technology of Taiwan, under the Contract Nos. MOST 106-2314-B-182 -062 -MY2 and108-2314-B-182 -029 -MY2

CONTACT INFORMATION

Email: hh.lin@mail.cgu.edu.tw